Available online at www.sciencedirect.com

ScienceDirect

Ceramics International 41 (2015) 2884–2891

CERAMICS INTERNATIONAL

www.elsevier.com/locate/ceramint

Formation and evolution of TiO_2 nanotubes in alkaline synthesis

Larisa B. Arruda[a], Cassio M. Santos[b], Marcelo O. Orlandi[c], Wido H. Schreiner[d], Paulo N. Lisboa-Filho[e,*]

[a]POSMAT – Programa de Pós-Graduação em Ciência e Tecnologia de Materiais UNESP, Bauru, Brazil
[b]UFC – Universidade Federal do Ceará, Departamento de Física, Fortaleza, Brazil
[c]UNESP – Univ Estadual Paulista, Instituto de Química, Departamento de Físico-Química, Araraquara, Brazil
[d]UFPR – Universidade Federal do Paraná, Departamento de Física, Curitiba, Brazil
[e]UNESP – Univ Estadual Paulista, Faculdade de Ciências, Departamento de Física, Bauru, Brazil

Received 22 August 2014; received in revised form 16 October 2014; accepted 19 October 2014
Available online 27 October 2014

Abstract

One-dimensional nanostructures have been intensively studied, from the point of view of their synthesis and mechanics of formation, as well as their applications. Titanium dioxide nanoparticles have been demonstrated to be an effective multifunctional material, especially when the particle size is less than 50 nm. TiO_2 nanotubes with diameters of about 10 nm were synthesized by the alkaline route. The synthesized samples were then studied by X-ray diffraction (XRD), Fourier transform infrared spectroscopy (FT-IR), transmission electron microscopy (TEM) and X-ray photoelectron spectroscopy (XPS). Analyses revealed that the nanotubes were mainly composed of titanium and oxygen, with small amounts of sodium ions in the sample obtained at pH 7 and no sodium at pH 4. The nanotubes obtained showed multiple walls, with dimensions of 5 nm in diameter and about 200 nm in length. In addition, the formation of the nanotubes occurred from a single crystal of TiO_2 during the washing process.

Keywords: TiO_2 nanotubes; Directed growth; Alkaline synthesis; Morphology

1. Introduction

The emergence of a new generation of nanomaterials has exponentially increased the interest of groups involved in the developmental process of synthesis, modification and application of these materials in the most diverse areas. This interest is due to the different properties that nanomaterials have when compared to the same material in bulk form [1]. In particular, the importance of physicochemical properties such as size, shape and surface modification of nanomaterials in biological effects has also been highlighted [2].

TiO_2 nanostructures have been the subject of intense research from the point of view of their synthesis and mechanisms of formation as well as their applications, such as in photocatalysis, solar cells, gas sensors, hydrogen storage and nanobiomaterials. This variety of applications is due to their chemical stability, non-toxicity and high refractive index. Also, since they are an n-type semiconductor with oxygen vacancies as the main type of dopant [3,4]. TiO_2 has a low electrical resistivity due to an increase in these vacancies, making it a potential candidate for oxygen sensors [5]. Among the several nanostructures (e.g., nanoparticles, nanotubes, nanowires, nanorods and nanofilms), tubular materials feature hollow structures and high surface-to-volume ratio [6]. These characteristics may also contribute to improving the reaction/interaction between a device and the surrounding medium, thereby making the system more effective or even allowing novel reaction pathways [7].

The synthesis of TiO_2 nanotubes can be carried out by three main methods: template-assisted, anodic oxidation and alkaline hydrothermal [8]. Hydrothermal processes are simple regarding the experimental procedure and less expensive, but evidence shows that the nanotubes formed are not only TiO_2 but also titanates. In many cases titanates such as $H_2Ti_5O_{11}•H_2O$ [9], $H_2Ti_2O_5•H_2O$

*Corresponding author. Tel.: +55 14 31036072; fax: +55 14 310306094.
E-mail address: plisboa@fc.unesp.br (P.N. Lisboa-Filho).

http://dx.doi.org/10.1016/j.ceramint.2014.10.113
0272-8842/

[10], $H_2Ti_4O_9•H_2O$ [11], $H_2Ti_3O_7$ and $Na_xH_{2-x}Ti_3O_7$ [12], among others, can coexist or be the predominant phase in the final synthesis product. Titanate nanotubes can be of great importance, considering that they show low absorption in the visible region and have a lower rate of recombination of photogenerated electron/hole pairs when compared with TiO_2 [5]. They are therefore considered as nanostructures that can have a significant impact on the development of new photoactive materials of high efficiency.

Since the discovery of alkaline synthesis for the formation of TiO_2 nanotubes by Kasuga [12] other works have been presented with similar synthetic routes, with small variations in time, temperature and alkaline medium during the process. Although there are numerous explanations for the formation process of nanotubes using alkaline medium, this route still generates controversies in the scientific community. Most works report that the formation of TiO_2 nanotubes occurs similarly to that of carbon nanotubes, where after the formation of TiO_2 nanosheets the rolling process occurs until the formation of TiO_2 nanotubes [8,13–15].

Lu et al. [8] further suggested that early in the synthesis, larger structures are formed resulting from the coalescence of smaller particles of TiO_2. After this first stage there is more irregular exfoliation of nanosheets from the crystals, forming spiral structures, reaching their lowest thermodynamic energy. Since the rolling time is less than that of the coalescence process of the particles, longer times of synthesis allow higher yields of nanotubes. Nakahira et al. [16] studied the relationship of hydrothermal synthesis time in NaOH medium and discovered that nanotubes began to form within a synthesis time of 3 h, reaching a maximum yield after 96 h. The authors proposed that sodium titanate nanosheets are formed on the surface of TiO_2 particles and, after curling, are retrieved with washing in HCl solution, important to provide exchange of Na^+ ions with H^+.

Another approach to the process of TiO_2 nanotube formation was proposed by Kukovez et al. [17], where the growth of these nanostructures occurs from TiO_6 oriented crystals even during the alkali treatment. According to Kukovez et al., even if the starting materials recrystallize in the form of titanate nanosheets, these do not become nanotubes, but the oscillations of local concentrations on the surfaces of the crystal lead to the formation of nanoloops from anatase starting materials, thereby providing the seeds for the process of oriented crystal growth and consequently leading to the formation of titanate nanotubes.

As can be seen, most authors argue that the formation of TiO_2 nanotubes or titanates occurs from the formation of sheets with their subsequent curling still during alkaline synthesis. In the present study two alkaline syntheses at atmospheric pressure were proposed, similar to that by Kasuga [13] but differing in the final pH of the wash, where a morphological and structural study was conducted focusing on the synthesis process, from the initial product until the formation of the tubes.

2. Experimental details

The samples in the study were prepared by mixing 12 g anatase TiO_2 (Aldrich, 99%) in 200 ml of 10 M NaOH. This mixture was kept at 120 °C for 24 h in a Teflon open container, which was placed in a glycerin bath, using a mantle heater for heating. The syntheses were carried out at ambient pressure, where only precursor reagents were subjected to alkaline treatment. After the alkaline treatment, the mixture was washed with 0.1 M hydrochloric acid (HCl) and deionized water (DW) repeatedly to remove the sodium ions. Samples with final neutral pH and final pH of 4 were separated for study, resulting in samples TpH-7 and TpH-4, respectively. Finally, the materials obtained were dried in a conventional oven at 200 °C for 24 h in air atmosphere. Also, during the synthesis of sample TpH-7, aliquots of the solution were removed to study the formation of nanotubes, where all aliquots were dried at room temperature. The group of samples and the description of each are given in Table 1.

Crystallographic phases were traced in a Rigaku D/MAX 2100PC conventional diffractometer. The voltage and the applied current used were 40 kV and 20 mA, respectively. The data were collected for scattering angles (2θ) ranging from 5° to 80° with a step of 0.02° for 1 s. Transmission electron microscopy (TEM) images were obtained with a Philips microscope, model CM200. Energy dispersive X-ray spectroscopy analyses were performed using a VGESCA LAB MK-2 surface analysis system with an electron energy analyzer and a dual Mg/Al anode X-ray source. Emission current of 24 mA and filament current of 5 A were used. XPS wide scan surveys were carried out in the range of 0–1100 eV with a step size of 1 eV and Al kα filament. Fourier transform infrared spectroscopy (FT-IR) spectra of the samples were obtained on a Bruker FT-IR spectrometer, model Vertex 70, at a resolution of 4 cm^{-1} and 32 scans with range of $4000-350\ cm^{-1}$ in the attenuated total reflectance mode (ATR) with diamond crystal and angle of incidence of 45°.

3. Results and discussion

A comparative study by XRD powder patterns obtained after each washing procedure is shown in Fig. 1. X-ray measurements revealed that the sample obtained after alkaline treatment, TpH-7A, showed no TiO_2 phase but the formation of a mixture of titanate with other products. The phases Na_2TiO_3 (PDF 47–130), NaO_3 (PDF 18-1235) and NaOH (PDF 78-189) were identified. After the first wash with deionized water, the TiO_2 phase (PDF 84-1286) appeared, as shown in the TpH-7B plot. $H_2Ti_2O_5•H_2O$ (PDF 47-0124) titanate was formed along with anatase TiO_2. With alternating washes of samples with DW and HCl solution, the crystallographic phase containing sodium ions was eliminated as

Table 1
Description of samples in study.

Sample	Description
TiO_2	Anatase (Aldrich 99.9%) commercial sample
TpH-7A	After alkaline treatment/dried at room temperature
TpH-7B	Washed with DW and dried at room temperature
TpH-7C	Washed with 0.1 M HCl/dried at room temperature
TpH-7D	Brought to neutral pH/dried at room temperature
TpH-7	After alkaline treatment/dried 200 °C/24 h – pH 7
TpH-4	After alkaline treatment/dried 200 °C/24 h – pH 4

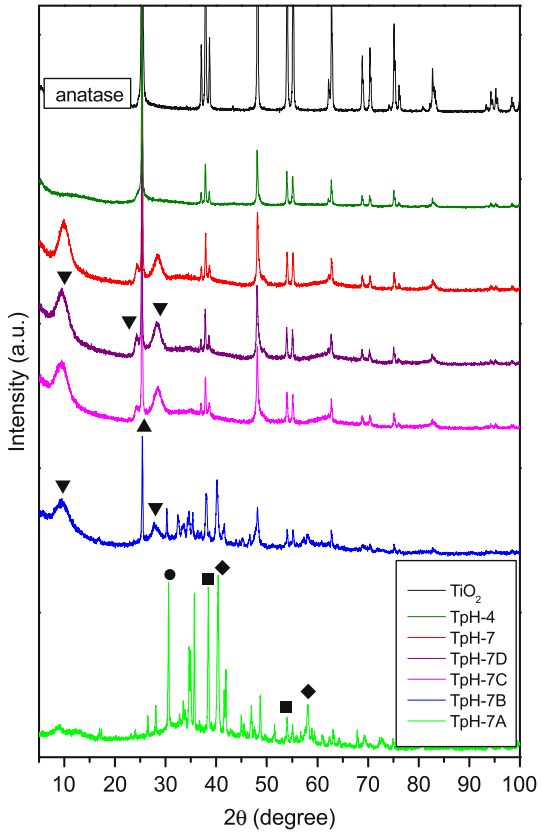

Fig. 1. XRD patterns of the products obtained from anatase with 10 M NaOH. With◆Na_2TiO_3 (PDF 47-130), ■ NaOH (PDF 78-189), ● NaO_3 (PDF 18-1235), ▼ $H_2Ti_2O_5•H_2O$ (PDF 47-0124) and ▲ anatase TiO_2 (PDF 84-1286).

shown in the curves of the TpH-7C and TpH-7D samples (Fig. 1). However, until neutralization of the medium, $H_2Ti_2O_5•H_2O$ titanate remained present, as seen in the XRD powder pattern for the TpH-7 sample.

It is therefore evident that the formation of the desired phase of TiO_2 structures occurred during washing processes with water and HCl solution with elimination of residual sodium ions, which were released into the medium and removed by centrifugation and not during alkaline treatment as found in earlier studies [16,17]. The complete elimination of all sodium and hydrogen titanates was possible only with a final pH of 4, which yielded the anatase TiO_2 phase, as shown in curve TpH-4.

XPS analyses confirmed the presence of sodium ions during all stages of the synthesis process for the sample with a final pH of 7. Fig. 2 shows the survey spectrum for sample TpH-7, where characteristic peaks of Na2s and Na1s are present at 36.3 and 1070 eV, respectively, probably due to the presence of amorphous NaOH. However, when the final pH was 4, these sodium ions were absent as noted by the survey spectrum in Fig. 3, confirming that all sodium ions were removed during washing. The Na KLL, O KLL and Ti LMM peaks are the corresponding Auger peaks [18].

It was also possible to observe the occurrence of a shift in the Ti2p peak to lower energies as shown in Fig. 4. The standard sample, which did not undergo any alkaline treatment, had peaks around 460 and 466 eV for $Ti2p_{3/2}$ and $Ti2p_{1/2}$, respectively. The

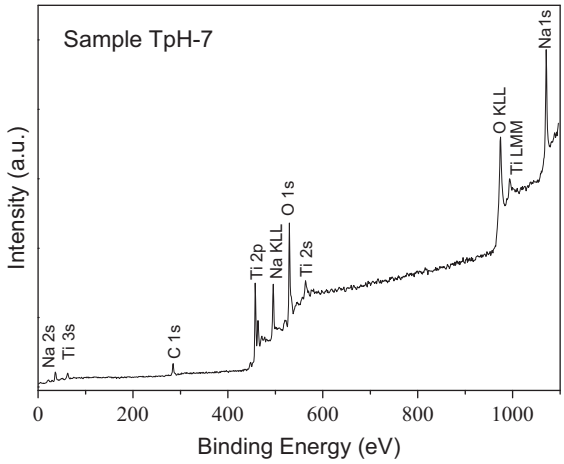

Fig. 2. XPS survey of the TpH-7 sample formed for TiO_2 nanotubes and nanotubular titanate.

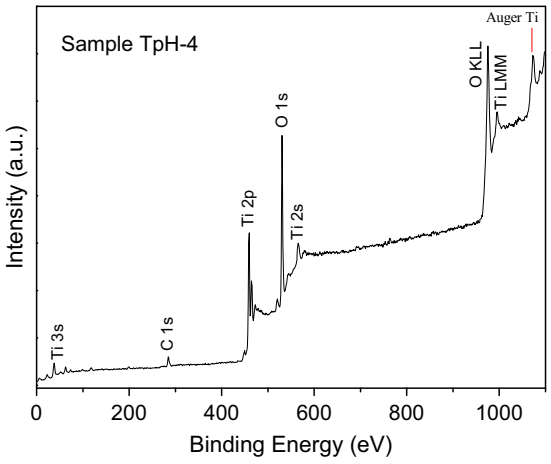

Fig. 3. XPS survey for the TpH-4 sample formed for TiO_2 nanotubes in the absence of titanates.

sample TpH-7, containing traces of sodium after the synthesis process, showed energy shifts of 457.7 and 463.8 eV.

In the TpH-4 sample, which was washed at a final pH of 4, there was no evidence of sodium ions, where these photoelectric peaks were near that of the standard sample with 459.7 eV for $Ti2p_{3/2}$ and 464.6 eV for $Ti2p_{1/2}$. This change in binding energy to lower values may have resulted from the formation of oxygen vacancies due to the breaking of Ti–O–Ti bonds in the TiO_6 octahedrons when the TiO_2 was subjected to alkaline treatment in NaOH medium. Also, the products formed during alkaline treatment and subsequent washings showed significant variation in the lengths of the Ti–O bonds [18,19].

The set of samples was also analyzed by FT-IR spectroscopy to study the structural changes during the synthesis of the nanotubes, and the spectra are shown in Fig. 5a. The broad band between 3750 and 2200 cm^{-1} corresponded mainly to contributions of OH. At 3587 cm^{-1}, it is possible to observe OH groups due to the stretching modes of Ti–OH [20]. The overlapping bands around 3400 and 3100 cm^{-1} are related to OH stretching modes from final multilayer molecular arrangements of H-bonded water [9,16],

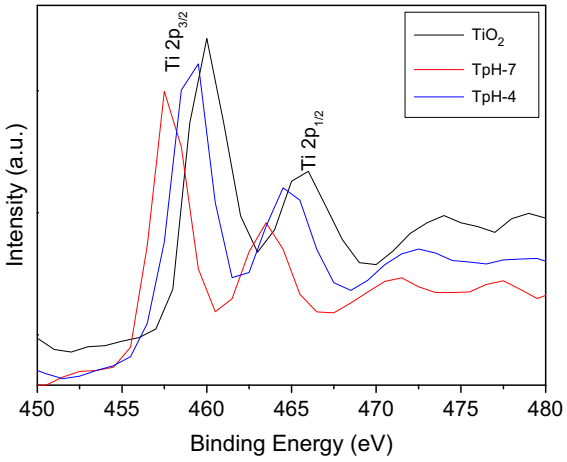

Fig. 4. XPS measurements showing shift of Ti2p peaks in Ti2p spectrum.

which decrease with washings and disappear when the samples are dried to obtain the final samples. Bands around 2500 and 2950 cm^{-1} were due to residual H_2O. Bands at 2906 and 2337 cm^{-1} indicated CO_2 and C–H bonds, respectively.

The 1637 cm^{-1} band was assigned to the bending mode of the water molecule including hydroxyl groups on the surface of titania [21,22], which also decreased with the drying process. Absorptions at 1450 cm^{-1} and 870 cm^{-1} could be assigned to the stretching mode of CO_3^{2-} groups. Also, the formation of Ti–OH groups during alkaline synthesis could be demonstrated at 1100 cm^{-1} [23].

As shown by XRD measurements the formation of the TiO_2 phase started to occur after the first wash with water, where the band at around 430 cm^{-1} showed the stretching vibration of the Ti–O bond [24], making the TiO_2 formation step clear, which was maintained until the final process in obtaining the samples.

A deconvolution of the FT-IR spectroscopy curve for the TpH-7A sample in the range from 4000 to 2100 cm^{-1} is proposed in Fig. 5b. As can be seen it is possible to identify six contributions, the most important being at 3295 cm^{-1} and 3587 cm^{-1}, the first related to the OH group in the terminal position of H_2O and the second related to OH groups in terminal position due to stretching of Ti–OH bonds, indicating the formation of titanates at this stage of the synthesis. Other bands at 2337 and 2906 cm^{-1} are related to CO_2 group and axial stretch C–H respectively. Furthermore the bands at 2500 and 2687 cm^{-1} can be assigned to OH stretch, which is not of fundamental importance to this particular study.

TEM analyses were performed to observe morphological changes at each step of the alkaline synthesis and to have a better knowledge about the formation of nanotubes. The micrographs in Fig. 6 show the sequence of aliquots for samples with pH 7.

The first aliquot taken after 24 h of alkaline treatment in NaOH medium showed a predominance of rounded particles with a mean diameter of 500 nm coexisting with ribbons connected to common points as shown in the micrographs in Fig. 6a and b, where these sheets had a maximum width of 500 nm and varying lengths. The first wash in water, after

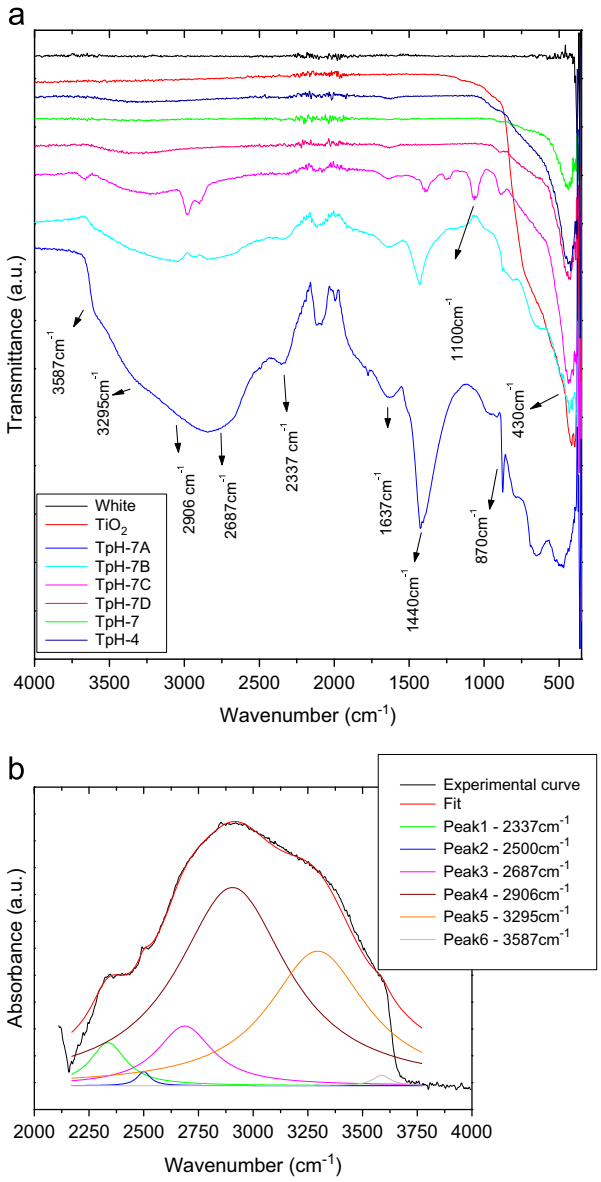

Fig. 5. (a) FT-IR spectra of the samples studied showing elimination of products formed during synthesis up to the final formation of TiO_2. Ti–OH groups are observed at 1100 cm^{-1} and decrease with washing, turning into Ti–O bonds around 450 cm^{-1}. (b) FT-IR deconvolution spectra for the TpH-7A sample in the range from 4000 to 2100 cm^{-1}.

alkaline treatment, favored a morphological change. As seen in Fig. 6c and d, thin sheets seem to grow from a common nucleus (like a flower) up to where they reach an unstable size and are then released, leaving only the loose sheets. At this stage, the spheres were no longer observed and could have been transformed into nanosheets or removed after centrifugation. The next stage of the synthesis consisted of acid washing the sample with HCl solution. As shown in the micrographs in Fig. 6e and f, nanotubes with an average diameter of 10 nm were formed in this step with the rolling of the sheets. However, as observed in X-ray measurements for the TpH-7 sample, these nanotubes were formed by not only TiO_2 but also hydrogen titanate, $H_2Ti_2O_5 \bullet H_2O$. Therefore, it is possible to affirm that the formation of nanotubes does not occur during

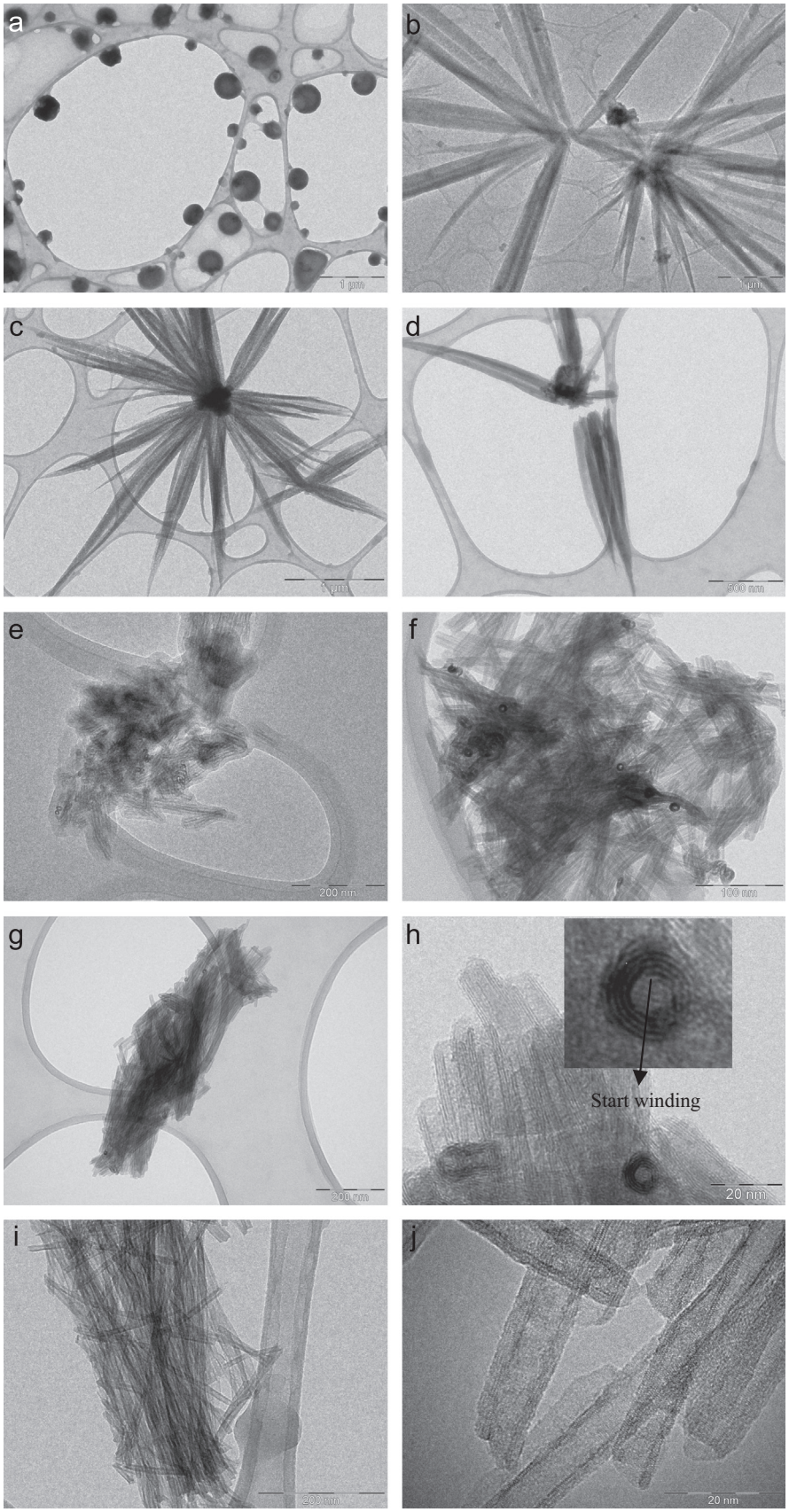

Fig. 6. Micrographs of the morphological evolution of sample TpH-7. (a,b) TpH-7A, after alkaline treatment. (c,d) TpH-7B, DW wash. (e,f) TpH-7C, HCl (0.1 M) wash. (g,h) TpH-7D, with neutral pH. (i,j) TpH-7, after alkaline treatment and drying at 200 °C for 24 h.

alkaline synthesis but during the washing process after removal of sodium ions. The micrographs in Fig. 6g and h show complete formation of the nanotubes after successive washings until obtaining a neutral pH. Thermal treatment at 200 °C for 24 h for removal of the liquid portion and obtaining the final powder had no influence on tube morphology as seen in Fig. 6i and j. As a result, nanotubes were formed with spiral-like walls and an outside diameter of 10 nm. In detail, Fig. 6h clearly shows the start of the coiled sheet resulting in nanotubes with various walls but all originating from a single sheet. This morphology was predominant in the samples studied.

Fig. 7 shows that some tubes from sample TpH-7 have an amorphous layer around it. This layer could have originated from products containing sodium ions remaining from the synthesis process in agreement with the XPS analyses. The formation of pure TiO_2 nanotubes was possible by increasing the number of washings until the solution reached a pH of 4, thus causing the removal of sodium ions as shown by XPS measurements, but maintaining the TiO_2 phase and nanotubular structure as observed by X-ray and TEM, respectively.

Although nanotubes could be obtained at different pH, the presence of sodium ions was shown to favor a more regular formation of nanostructures than when only TiO_2 nanotubes were synthesized. Fig. 8a and b shows that sample TpH-7 consists of more homogeneous nanotubes compared with sample TpH-4, which has nanotubes with irregular walls, as shown in Fig. 8c and d.

When subjected to alkaline treatment, the Ti–O–Ti bonds are broken, resulting in Ti–O–Na and Ti–OH bonds [12,25]. The formation of these new intermediate bonds causes distortions in the TiO_6 octahedrons due to differences in the lengths of the bonds. According to Nosheen [18] a rearrangement of bonds occurs in a layered structure by sharing the edges of the distorted octahedral of TiO_2, where Na and OH ions are intercalated between these layers. Accordingly, the alkaline environment causes the dissolution of TiO_2 followed by recrystallization of titanates, together with the formation of TiO_2.

Lee et al. [26] produced titanate nanotubes by the hydrothermal technique also in the presence of sodium hydroxide solution followed by washes using different concentrations of hydrochloric acid and observed that the titanate nanotubes were destroyed only in the absence of sodium. Tests carried out by Lee and collaborators showed that the nanotubular structure could be destroyed if the concentration of HCl used in the washing step was greater than 0.01 M. Lee suggests that it is also possible that sodium is coordinated with water molecules trapped within the interlayer space after hydrothermal synthesis. Therefore, we can say that the removal of sodium not only led to the breaking of the Ti–O–Na bonds but also caused a change in the sheet surface generating a surface irregularity that was more evident at the end of the rolling of the sheets and final formation of the tubes as shown in Fig. 8c and d.

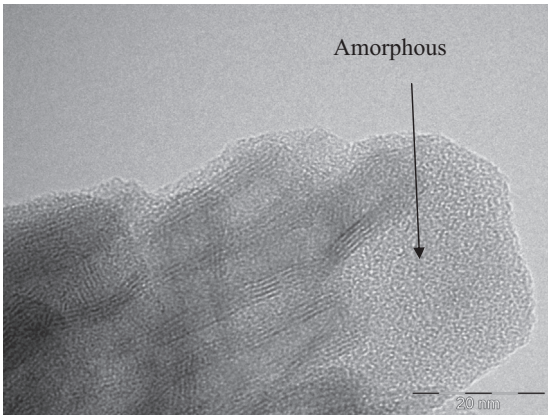

Fig. 7. $TiO_2/H_2Ti_2O_5{\bullet}H_2O$ nanotubes wrapped by amorphous material.

Perturbations and distortions in the lattice caused by chemical reactions due to the highly basic medium are very important for the formation of nanotubes, and the presence of sodium ions in octahedral structures consequently helps to obtain regular nanostructures as observed in the micrographs in Fig. 8a and b. In the case of sample TpH-4, the excess washes to remove sodium ions caused morphological changes distinct from those observed with sample TpH-7. Nevertheless, the dimensions of the nanotubes remained similar with diameters around 10 nm.

Although the diameter of the nanotubes was similar in both cases, the thickness of walls changed significantly. Samples with pH 7 nanotubes had an internal diameter of approximately 4.0 nm, while for pH 4 there were thinner walls of about 2.4 nm, similar to the nanotubes obtained by Liu et al. [4]. The interlayer distance also showed significant changes, with values of 0.74 nm for the pH 7 samples and 0.34 nm for the pH 4 samples, corresponding to the planes of anatase structure (001) and (101), respectively [14,27].

Thus, evidence showed that the synthesis method used resulted in nanotubes from nanosheet growths of particles formed during the washing process. TiO_2 or hydrogen titanate nanotubes could be obtained by the same method by varying only the final pH of the samples.

4. Conclusions

TiO_2 and hydrogen–titanate nanotubes were successfully prepared by a simple synthesis in alkaline medium at ambient pressure, and their morphological evolution was studied step by step during the synthesis process. These nanotubes were around 10 nm in diameter and 200 nm in length with different interplanar distances. For samples with a final pH of 7 in the presence of hydrogen titanate there was a growth in the plane (001), while for anatase TiO_2 samples with a final pH of 4, growth was in the plane (101). Also the washing process is important for the removal of accumulating sodium ions from the basic medium, where these ions have an essential role in the formation of the structures due to the variation in the distances of bonds when Ti–O–Ti bonds are broken to rearrange the bonds with Na^+ or OH^-. It was found that the formation of nanotubes occurred during the washing process in acid and not during the initial alkaline treatment. Furthermore, the study by transmission electron microscopy showed that the formation of nanotubes occurred from sheets initially linked to the nuclei of round particles formed in the alkaline synthesis. Thus, we highlight three important morphologies of this synthesis: round

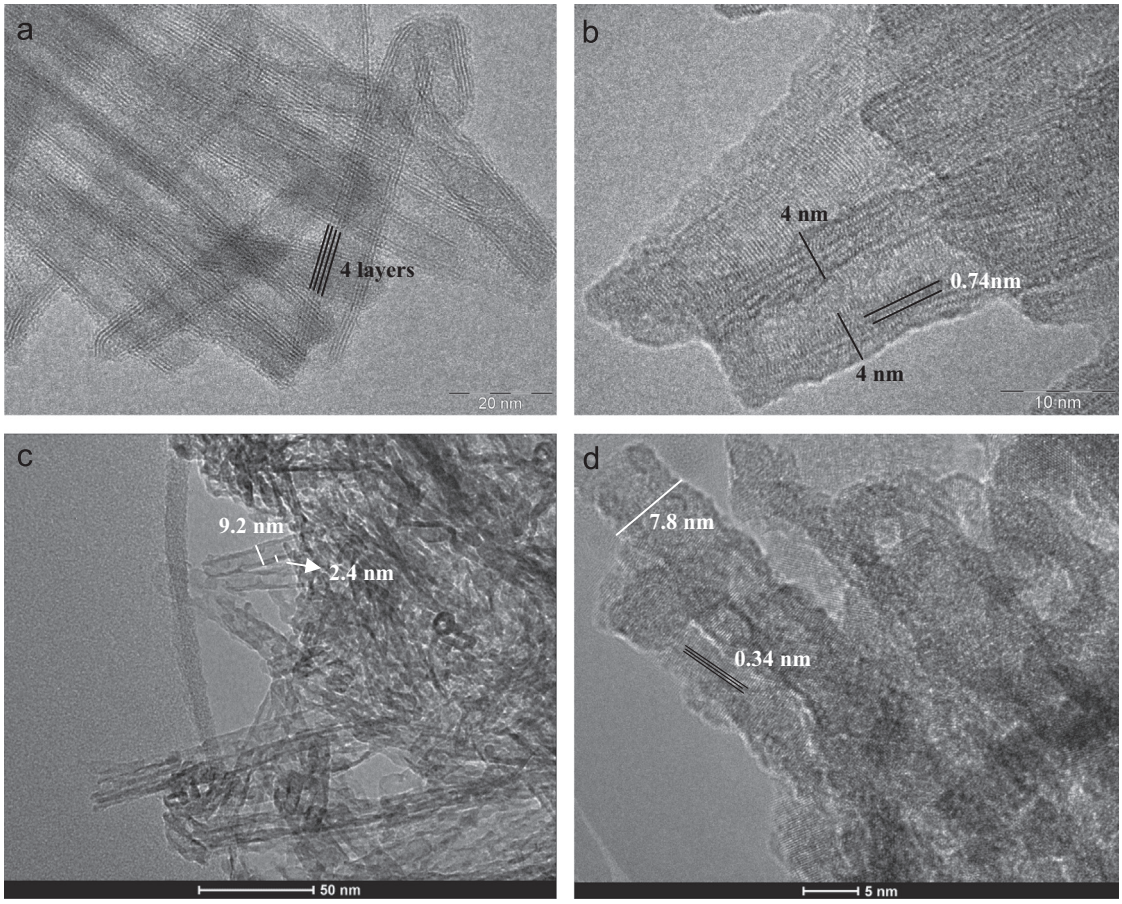

Fig. 8. Comparison of the morphologies of the nanotubes obtained at different pH. (a,b) pH 7 and (c,d) pH 4

particles followed by growth of thin sheets and nanotubes formed from a single rolled sheet.

Acknowledgment

The authors wish to thank the Brazilian agencies FAPESP (Research project 2011/22098-7) and CNPq (304810/2010-0) for financial support. Dr. A. Leyva helped with English editing of the manuscript.

References

[1] L.C. Cheng, X. Jiang, J. Wang, C. Chen, R.S. Liu, Nano–bio effects: interaction of nanomaterials with cells, Nanoscale 5 (2013) 3547–3569.
[2] S. Chibber, S.A. Ansari, R. Satar, New vision to CuO, ZnO, and TiO_2 nanoparticles: their outcome and effects, J. Nanopart. Res. 15 (2013) 1492, 1–13.
[3] B.J. Morgan, G.W. Watson, Determination of a morphological phase diagram of titania/titanate nanostructures from alkaline hydrothermal treatment of degussa P25, J. Phys. Chem. C 114 (2010) 2321–2328.
[4] F. Liu, L. Lu, P. Xiao, H. He, L. Qiao, Y. Zhang, Effect of oxygen vacancies on photocatalytic efficiency of TiO_2 nanotubes aggregation, Bull. Korean Chem. Soc. 33 (2012) 2255–2259.
[5] T. Kida, M.H. Seo, K. Suematsu, M. Yuasa, Y. Kanmura, K. Shimanoe, A micro gas sensor using TiO_2 nanotubes to detect volatile organic compounds, Appl. Phys. Express 6 (2013) 047201–047203.
[6] X. Meng, M.N. Banis, D. Geng, X. Li, Y. Zhang, R. Li, H. Abou-Rachid, X. Sun, Controllable atomic layer deposition of one-dimensional nanotubular TiO_2, Appl. Surf. Sci. 266 (2013) 132–140.
[7] P. Roy, S. Berger, P. Schmuki, TiO_2 nanotubes: synthesis and applications, Angew. Chem. 50 (2011) 2904–2939.
[8] H. Lu, J. Zhao, L. Li, J. Zheng, L. Zhang, L. Gong, Z. Wang, Z. Zhu, A systematic study on evolution mechanism of titanate nanostructures in the hydrothermal process, Chem. Phys. Lett. 508 (2011) 258–264.
[9] Z.Y. Yuan, B.L. Su, Titanium oxide nanotubes, nanofibers and nanowires, Colloids Surf. A: Physicochem. Eng. Aspects 241 (2004) 173–183.
[10] P. Haro-González, M. Pedroni, F. Piccinelli, L.L. Martín, S. Polizzi, M. Giarola, G. Mariotto, A. Speghini, M. Bettinelli, I.R. Martín, Synthesis, characterization and optical spectroscopy of Eu^{3+} doped titanate nanotubes, J. Lumin. 131 (2011) 2473–2477.
[11] C. Huang, K. Zhu, M. Qi, Y. Zhuang, C. Cheng, Preparation and photocatalytic activity of bicrystal phase TiO_2 nanotubes containing TiO_2-B and anatase, J. Phys. Chem. Solids 73 (2012) 757–761.
[12] T. Kasuga, Formation of titanium oxide nanotubes using chemical treatments and their characteristic properties, Thin Solid Films 496 (2006) 141–145.
[13] Dmitry V Bavykin, Frank C Walsh, Titanate and Titania Nanotubes, first ed., RSC Publishing, London, 2010.
[14] A. Turki, H. Kochkar, C. Guillard, G. Berhault, A. Ghorbel, Effect of Na content and thermal treatment of titanate nanotubes on the photocatalytic degradation of formic acid, Appl. Catal. B—Environ. 138-139 (2013) 401–415.
[15] M. Safaei, R. Sarraf-Mamoory, M. Rashidzadeh, The interactive effect of agitation condition and titania particle size in hydrothermal synthesis of titanate nanostructures, J. Nanopart. Res. 12 (2010) 2723–2728.
[16] A. Nakahira, T. Kubo, C. Numako, Formation mechanism of TiO_2-derived titanate nanotubes prepared by the hydrothermal process, Inorg. Chem. 49 (2010) 5845–5852.

[17] A. Kukovecz, M. Hodos, E. Horváth, G. Radnóczi, Z. Kónya, I. Kiricsi, Oriented crystal growth model explains the formation of titania nanotubes, J. Phys. Chem. B 109 (2005) 17781–17783.
[18] S. Nosheen, F.S. Galasso, S.L. Suib, Role of Ti–O bonds in phase transitions of TiO_2, Langmuir. 25 (2009) 7623–7630.
[19] M.A. Khan, H.T. Jung, O. Yang, Synthesis and characterization of ultrahigh crystalline TiO_2 nanotubes, J. Phys. Chem. B 110 (2006) 6626–6630.
[20] R. Camposeco, S. Castillo, I. Mejia, V. Mugica, R. Carrera, A. Montoya, M. Morán-Pineda, J. Navarrete, R. Gómez, Active TiO_2 nanotubes for CO oxidation at low temperature, Catal. Commun. 17 (2012) 81–88.
[21] T. Gao, H. Fjellvag, P. Norby, Crystal structures of titanate nanotubes: a Raman scattering study, Inorg. Chem. 48 (2009) 1423–1432.
[22] A. Rendón-Rivera, J.A. Toledo-Antonio, M.A. Cortés-Jácome, C. Angeles-Chávez, Generation of highly reactive OH groups at the surface of TiO_2 nanotubes, Catal. Today 166 (2011) 18–24.
[23] P. Zhang, Z. Zhang, W. Li, M. Zhu, Effect of Ti–OH groups on microstructure and bioactivity of TiO_2 coating prepared by micro-arc oxidation, Appl. Surf. Sci. 268 (2013) 381–386.
[24] Z. He, W. Que, J. Chen, Y. He, G. Wang, Surface chemical analysis on the carbon-doped mesoporous TiO_2 photocatalysts after post-thermal treatment: XPS and FTIR characterization, J. Phys. Chem. Solids 74 (2013) 924–928.
[25] C.L. Wong, Y.N. Tan, A.R. Mohamed, A review on the formation of titania nanotube photocatalysts by hydrothermal treatment, J. Environ. Manage. 92 (2011) 1669–1680.
[26] C.K. Lee, C.C. Wang, L.C. Juang, M.D. Lyu, S.H. Huang, S.S. Liu, Effects of sodium content on the microstructures and basic dye cation exchange of titanate nanotubes, Coll. Surf. A: Physicochem. Eng. Aspects 317 (2008) 164–173.
[27] M.A. Khan, Hee-Tae Jung, O-Bong Yang, Synthesis and characterization of ultrahigh crystalline TiO_2 nanotubes, J. Phys. Chem. B 110 (2006) 6626–6630.